Changes in seismicity and stress loading on subduction faults in the Kanto region, Japan, 2011–2014

Blandine Gardonio, David Marsan, Olivier Lengliné, Bogdan Enescu, Michel Bouchon, Jean-Luc Got

AGU PUBLICATIONS

JGR

Journal of Geophysical Research: Solid Earth

RESEARCH ARTICLE

10.1002/2014JB011798

Key Points:
- Seismicity activity increased in Kanto after 2011
- Repeating earthquakes show relaxing rate on the Philippine sea plate since 2011
- The updip locked portion of the PHS plate has remained less affected

Supporting Information:
- Figures S1 and S2

Correspondence to:
B. Gardonio,
blandine.gardonio@ujf-grenoble.fr

Citation:
Gardonio, B., D. Marsan, O. Lengliné, B. Enescu, M. Bouchon, and J.-L. Got (2015), Changes in seismicity and stress loading on subduction faults in the Kanto region, Japan, 2011–2014, *J. Geophys. Res. Solid Earth*, *120*, 2616–2626, doi:10.1002/2014JB011798.

Received 21 NOV 2014
Accepted 17 MAR 2015
Accepted article online 25 MAR 2015
Published online 30 APR 2015

Changes in seismicity and stress loading on subduction faults in the Kanto region, Japan, 2011–2014

Blandine Gardonio[1], David Marsan[1], Olivier Lengliné[2], Bogdan Enescu[3], Michel Bouchon[4], and Jean-Luc Got[1]

[1]ISTerre, Université de Savoie, CNRS, Le Bourget-du-Lac, France, [2]IPGS, CNRS, Université de Strasbourg, Strasbourg, France, [3]Earth Evolution Sciences Department, Faculty of Life and Environmental Sciences, University of Tsukuba, Tsukuba, Japan, [4]ISTerre, Université de Grenoble, CNRS, Grenoble, France

Abstract Seismic activity has increased in the Kanto region, Japan, following the 2011 *M*9.0 Tohoku earthquake. We here reassess this increase up to June 2014, to show that normal, Omori-like relaxation characterizes the activity on crustal faults as well as on the Philippine Sea plate, but not on the deeper Pacific plate. There repeating earthquakes display a twofold rate of occurrence (still ongoing in June 2014) as compared to the pre-Tohoku rate, suggesting enhanced creep. We compute the Coulomb stress changes on the upper locked portion of the Philippine Sea plate, which last ruptured in 1923. We find that this fault was little affected by either the coseismic, the postseismic, the accelerated creep, or the 2011 Boso silent slip event.

1. Introduction

The Kanto region that hosts Tokyo and its 25 million inhabitants is characterized by a double subduction: the Philippine Sea plate (PHS) subducts northward at shallow depth underneath the North American plate (NA) and the Pacific plate (PAC) dives beneath both PHS and NA at greater depth [*Ishida*, 1992; *Wu et al.*, 2007], cf. Figure 1a. The updip portion (depth z less than 20 km) of the PHS plate is known to be locked [*Sagiya*, 2004; *Nishimura et al.*, 2007] and to accumulate stress, its failure can cause destructive earthquakes, like the *M*7.9 Kanto earthquake that stroke the region in 1923. Kanto lies just off the 2011, *M*9.0 Tohoku rupture, although one of the biggest aftershocks, of magnitude *M*7.9, occurred off-coast Kanto, extending the megathrust rupture zone more to the south. The question as to whether the 2011 megathrust rupture and its aftershocks have hastened or not the future occurrence of a large earthquake in the Kanto region is of paramount importance, given the dense population and potential economic loss that would result from such a catastrophic event. Consequences of the Tohoku earthquake were studied in the Kamaichi area where an increase in repeating earthquakes magnitude was observed [*Uchida et al.*, 2015].

Toda and Stein [2013] observed an increase in seismicity after the 2011 shock in Kanto region, developing into a constant rate of earthquakes 2.9 times higher than the prior rate. This rate increase appears consistent with both positive changes in Coulomb stress resolved on deep portions of their proposed Kanto fragment, in particular, as well as with a clear tendency for Coulomb stress changes to be positive when computed using the focal mechanisms of earthquakes that occurred prior to the main shock [*Ishibe et al.*, 2011]. *Uchida and Matsuzawa* [2013] likewise document a ninefold increase compared to pre-Tohoku rate, in the rate of repeating earthquakes (their area 16) from April to December 2011, which marks the end of their analysis period. Also, *Hirose et al.* [2012] argued that the Tohoku earthquake hastened the occurrence of the recurrent slow slip event (SSE) off Boso, on the PHS plate. All these observations (see also *Somerville* [2014]) suggest that a significant increase in stress loading was brought up in the Kanto region by the 2011 main shock.

We here dwell on the study by *Toda and Stein* [2013] in order (i) to investigate how the change in seismicity has evolved with 18 extra months of data and (ii) to monitor time variations in creeping rate at depth on the PHS plate as evidenced by repeating earthquake time series and how this change in creep more particularly affected the locked updip portion of the PHS plate.

2. Changes in Seismicity Caused by the M_w9.0 Tohoku Earthquake

Toda and Stein [2013] observed changes in seismicity due to the Tohoku earthquake between 2009 and 2012 in the area delimited by the black rectangle in Figure 1b. They found that seismicity remained constant from

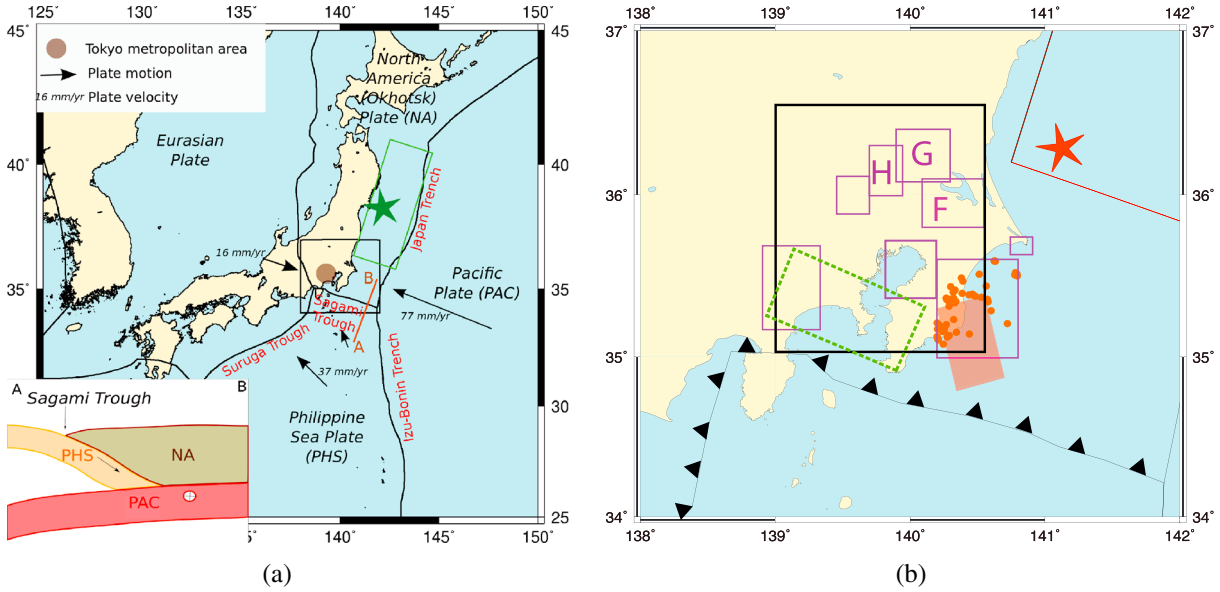

Figure 1. Tectonic settings of Japan. (a) Black rectangle showing the Kanto area. Box: Simplified view of the plates interaction with depth along the brown line AB (no scale). (b) Brown rectangle showing the source of the October 2011 slow slip event (SSE) in the Boso area [*Hirose et al.*, 2012], the brown dots represent the swarm earthquakes that accompanied it. The source of the 1923 Kanto earthquake [*Matsu'ura and Iwasaki*, 1983] is shown in green. The black rectangle delimits the area studied here. The red line shows the southern limit of the 2011 Tohoku rupture based on the locations of its immediate aftershocks, the red star is the epicenter of the *M*7.9 aftershock that occurred half an hour after the main shock. The purple boxes show the areas where repeating earthquakes have been observed for the 1979–2003 period [*Kimura et al.*, 2006; *Uchida et al.*, 2009]. We here study repeating earthquakes in areas F, G, and H of *Kimura et al.* [2006] only, for the 2004—2014 period.

the end of 2011 throughout the whole of 2012, suggesting that the loading of active portions of the megathrust faults in Kanto has reached a new, accelerated, steady rate. They were able to fit the time series with a rate-and-state model driven by Coulomb stress changes brought by both the *M*9.0 and its *M*7.9 aftershock, resolved on individual fault planes. To do so, they needed to raise the stress loading rate from 0.25 to 0.7 bar/year, hence, a 2.8 times increase. According to their study, this translates into a 2.5-fold increase of the estimated probability that a $M \geq 7.0$ earthquake will strike the region in the 5 years after the *M*9.0 main shock.

We analyze the updated Japan Meteorological Agency earthquake catalog spanning from January 2009 to June 2014 with newly added events after Tohoku, in the same area (black rectangle in Figure 1b), to show that, while the relaxation actually resumed after 2012, hence after the time period analyzed by *Toda and Stein* [2013], this relaxation is anomalously slow in the 30 to 85 km depth interval which characterizes subduction seismicity.

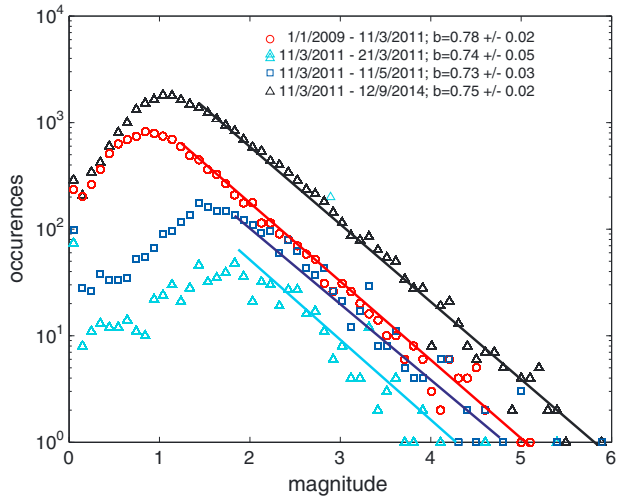

Figure 2. Number of earthquakes versus magnitude in the Kanto region (black box in Figure 1b), for the pre- and post-Tohoku periods. The magnitude of completeness is taken equal to 2.0 for the overall period.

Changes in earthquake rate over time are computed; in order to make sure that these changes do not come from a bias due to a change in magnitude of completeness M_c, we estimate the latter before and after the Tohoku earthquake, in the Kanto area (Figure 2). We find that M_c=1.5 for the 1 January 2009 to 11 March 2011 period and $M_c = 2.0$ after 11 March 2011. The latter M_c applies shortly after the main shock: $M \geq 2.0$ earthquakes are

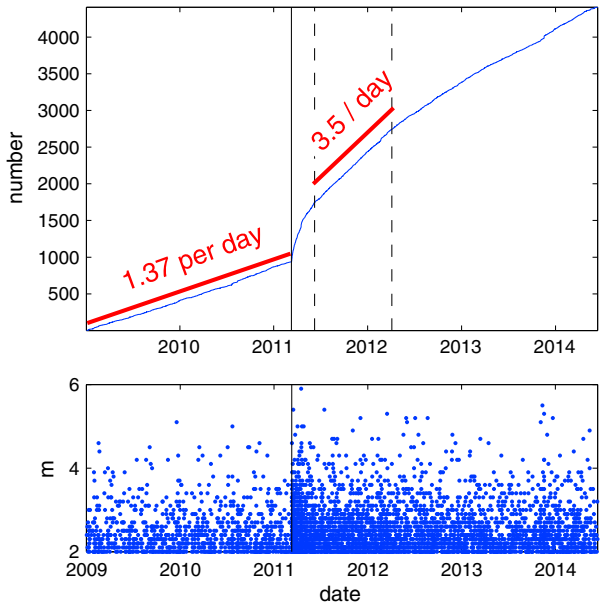

Figure 3. (top) Cumulative number of $M \geq 2$ earthquakes in the Kanto area located at depth between 0 and 100 km. The black line indicates the occurrence of Tohoku. (bottom) Magnitude versus time. The period characterized by a constant increased rate of 3.5 per day ended after about 300 days. A slow relaxation then resumed.

complete after 10 days past the main shock, and this period of completeness at $M_c = 2.0$ possibly extends even earlier in time, although the limited number of earthquakes then prevent us from being definite.

The seismicity rate in the area of Kanto is constant during the pre-Tohoku period (2009 to 11 March 2011) and then increases after the Tohoku earthquake until reaching a plateau after 90 days (Figure 3). This plateau lasts for about 300 days. This regime is coherent with the analysis of *Toda and Stein* [2013] and affects the whole of Kanto. However, we find that it did not last past this interval of 300 days; relaxation then resumed as normally expected. This observation is further confirmed when removing aftershocks from the data and calculating the background seismicity using the method of *Marsan et al.* [2013], see Figure 4.

All depth intervals do not show the same behavior (Figure 5). Crustal depths (0–30 km) undergo an increase of seismicity after the Tohoku earthquake that is well fitted by an Omori-Utsu law $\lambda(t) = K/(t+c)^p + \mu$, where λ is the earthquake rate and μ the pre-Tohoku rate; we find an exponent $p = 1.14$ by maximizing the likelihood for inhomogeneous Poisson statistics (red curve in Figure 5a), up to a second rate increase in October 2011 corresponding to the occurrence of a SSE in Boso [*Hirose et al.*, 2012, 2014]. The seismicity rate then resumes the pre-Tohoku value about 1 year after the main shock. An omori-Utsu decay is only asymptotic; we thus here use the 125% level, i.e., the rate equals 125% of the preseismic rate, to arbitrarily fix a characteristic time. We find that the fitted Omori-Utsu law is back to this 125% level after 408 days. Visually, the slope of Figure 5a after mid-2012 is indistinguishable from the pre-Tohoku rate. The seismicity then increases again due to a 1 week long swarm in the Boso area at the beginning of 2014.

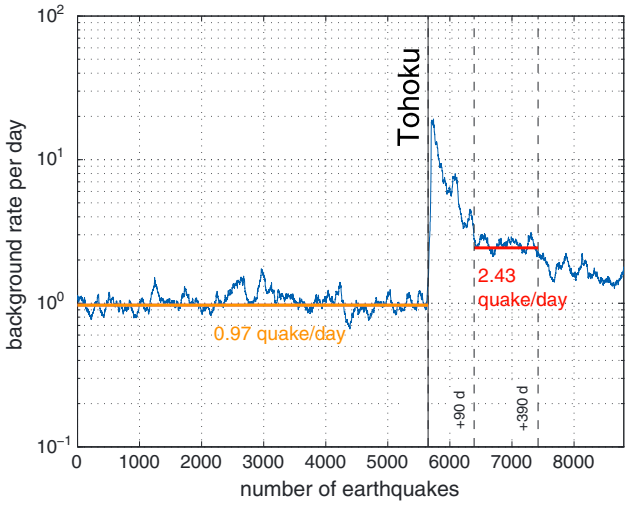

Figure 4. Background seismicity rate for $M \geq 2$ earthquakes computed with the method described in *Marsan et al.* [2013], again showing a transient regime with a constant background rate from +90 to +390 days after Tohoku, followed by further relaxation.

Between 30 and 85 km depth, a low p value of 0.71 is needed to fit the Omori-Utsu law (Figure 5b). This points to an anomalously slow relaxation of the stress imparted by the main shock and its M7.9 aftershock. Anomalously low p values were calculated by *Nanjo et al.* [2013] ($p = 0.44 \pm 0.09$ for M3 earthquakes up to 30 May 2012) and needed by *Toda and Stein* [2013] ($p = 0.44 \pm 0.07$ for M3 earthquakes) to model the seismicity in Kanto up to 2012 without changing the background rate. We calculated the p value needed for $M \geq 3$ earthquakes between 0 and 150 km in the area studied by Nanjo et al. and found that $p = 0.71$; this low value is the same as the one for $30 \leq z \leq 85$ km, owing to the fact that the seismicity is mostly found at subduction depths. This slow relaxation is here found to be valid up to June 2014, without any

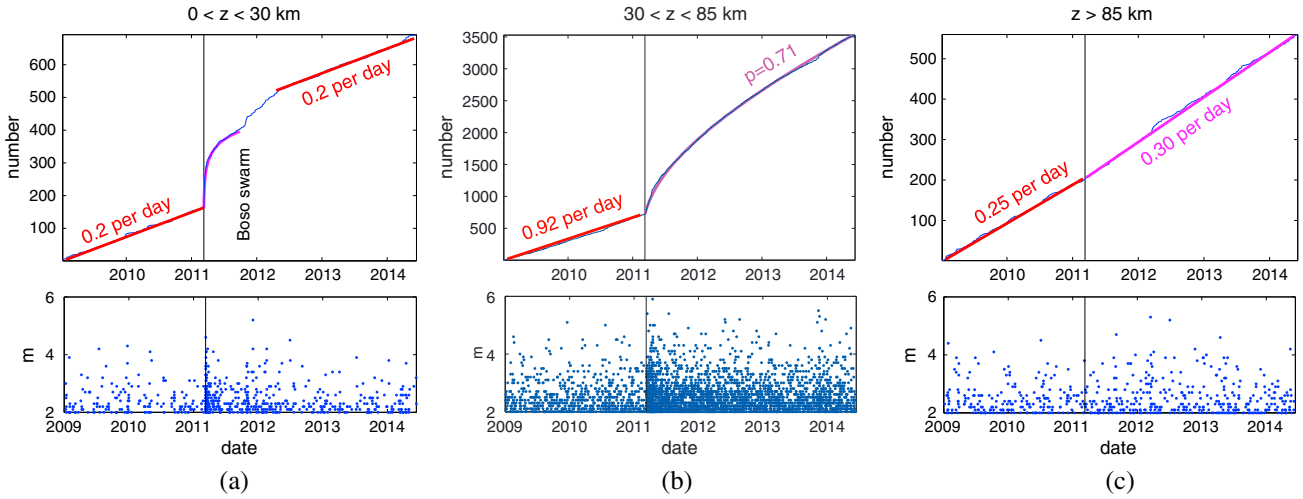

Figure 5. (top) Cumulative number of earthquakes for the Kanto area at crustal (0–30 km), intermediate (30–85 km), and greater depths ($z > 85$ km). Fits by a constant occurrence rate in the pre-Tohoku phase and by an Omori-Utsu law after the Tohoku earthquake are shown in color. (bottom) Magnitude versus time.

apparent departure from this trend and to only characterize subduction depths. The relaxation at these depths was still going on by June 2014; if it were to continue unchanged, the seismicity rate would reach 125% of the post-Tohoku rate after 19 years (i.e., in 2030).

To check how peculiar this slow relaxation is, we looked at the cumulative number of earthquakes in the northern part of Honshu for rectangular areas of 1° × 1° at subduction depths under the land. The only areas that show an increase in seismicity are the ones closest to the Tohoku earthquake epicenter (see supporting information). The rest of subduction seismicity underneath Honshu resumed the pre-Tohoku rate within less than 2 years, unlike Kanto where one can speculate about ongoing creep in the transition zone that potentially affects the loading of the updip PHS interface.

At greater depth ($z > 85$ km), the effect of the Tohoku earthquake is not as strong as for $30 < z < 85$ km (Figure 5c), at least for $M \geq 2.0$ earthquakes. We find a +18% increase in rate between the pre- and post-Tohoku periods, with both periods characterized by a nearly constant rate. The probability that the observed 357 earthquakes with $M \geq 3.0$ earthquakes after the main shock could be due to natural fluctuations in a homogeneous Poisson process with rate equal to the pre-Tohoku rate is 2.7×10^{-5}, implying that this rate change, although very moderate, is statistically significant. Furthermore, we checked that the observed +18% increase in seismicity is not due to a change of M_c.

Increased seismic activity in Kanto can be potentially linked to the local maximum in postseismic slip found from GPS inversion offshore Kanto [*Ozawa et al.*, 2011, 2012; *Perfettini and Avouac*, 2014]. This maximum is well evidenced by a change in direction of the surface displacement vectors between the coseismic and the postseismic phases. Using 512 GPS stations in central and northern Japan, we fit the measured postseismic displacements as $U(t) = a \times \log(1 + t/\tau) + b \times t$, where U is the displacement component (east, north, or up) and t is the time (in days) after the Tohoku earthquake, up to 22 September 2012. A least squares fit is performed from the first sample after Tohoku, accounting for the uncertainties in the displacement increments. We use the best fits to extrapolate the postseismic displacements up to 1 year after the main shock and plot them together with the coseismic displacements (Figure 6). The local slip maximum at depth is evidenced by GPS stations for which postseismic displacement is relatively strong and presents a clockwise rotation from the coseismic displacement direction. This local maximum could be partly explained by the occurrence of an SSE on Boso area right after Tohoku earthquake [*Kato et al.*, 2014] but also in October of the same year [*Hirose et al.*, 2012, 2014]. Viscoelastic relaxation was hypothesized close to Tohoku-oki rupture [*Watanabe et al.*, 2014; *Sun et al.*, 2014]; for the Kanto area, there is no evidence of such made of relaxation since the closest GPS seafloor station (CHOS) indicates a SE movement. We thus make the assumption that the GPS displacements are mostly due to afterslip for the Kanto area.

We conclude from this analysis of seismicity that, while crustal activity was only affected for about 1 year after the main shock, deep portions of the PAC and PHS subducting slabs exhibit changes that have not, so far, fully

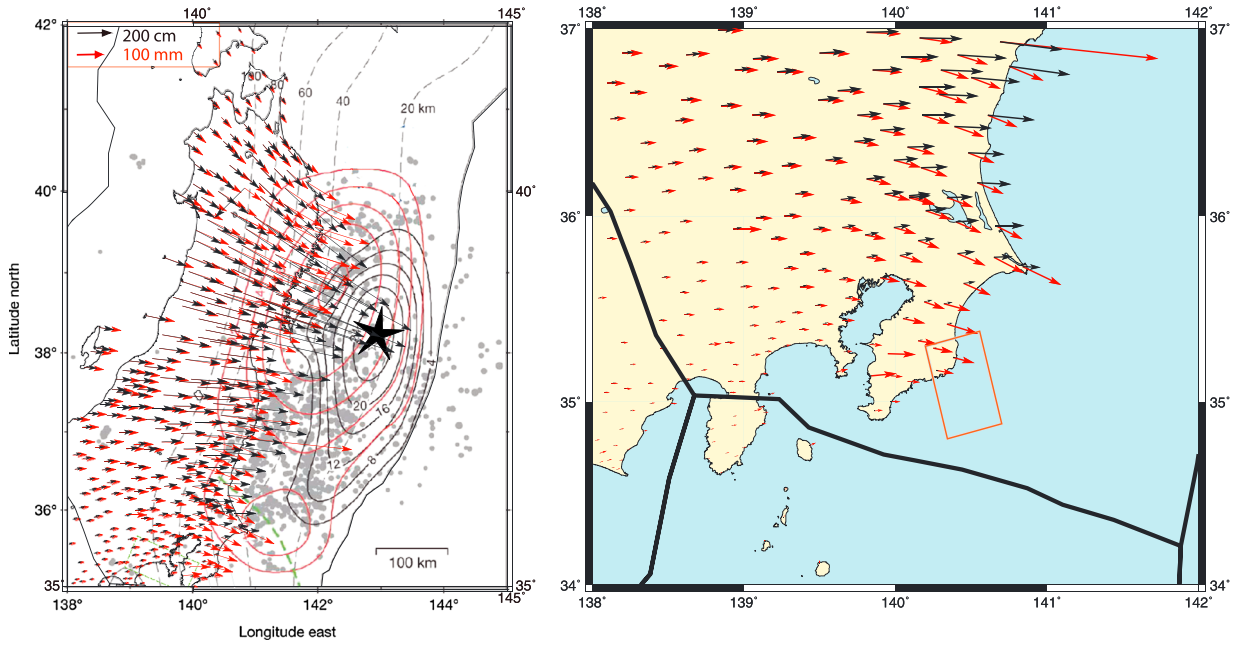

Figure 6. Coseismic (red arrows) and postseismic (black arrows) horizontal inland displacements along with estimated coseismic (red contour with 4 m interval) and postseismic slip (black contour with 0.2 m interval) on the PAC plate, after *Ozawa et al.* [2011] who studied postseismic slip from 12 to 25 March 2011. The black star is the Tohoku earthquake epicenter, and gray dots are aftershocks. The source of the October 2011 Boso SSE is shown in red rectangle [*Hirose et al.*, 2012]. (b) Zoom in on the Kanto area (black rectangle in Figure 6a). The reference point is the northernmost station in Hokkaido.

relaxed. In fact, the observed relaxation of activity in the 30–85 km depth range is anomalously slow (p exponent of 0.66, well below the typical 1.0 value). GPS displacements clearly suggest that off-rupture postseismic slip developed in Kanto after the Tohoku earthquake. This slip was potentially still going on in June 2014, as evidenced by seismicity. We now further investigate this particular depth range, by analyzing time series of repeating earthquakes occurring on both subducting plates, to resolve variations in creeping rate.

3. Repeating Earthquakes

Repeating earthquakes (REs) are earthquakes that break a common asperity with nearly identical rupture lengths. REs have been found in California, most notably on the Parkfield segment of the San Andreas Fault [*Nadeau et al.*, 1995], and in Japan [*Matsuzawa et al.*, 2002], including the Kanto region [*Kimura et al.*, 2006], as well as other parts of the world [e.g., *Chen et al.*, 2007; *Bouchon et al.*, 2011]. In order to repeatedly rupture the same fault patch, the stress-bearing asperity must be mechanically isolated to some extent from other neighboring asperities. The picture according to which these asperities are surrounded by a velocity-strengthening (i.e., creeping) fault zone has thus emerged. Departure from such a periodic, hence stationary, regime can reveal either stress interactions between asperities, changes in creeping rate, or complexity in the rupture process [*Schaff et al.*, 1998; *Nadeau and McEvilly*, 1999; *Lengliné and Marsan*, 2009; *Bouchon et al.*, 2011].

We here study the occurrence rate of REs in the Kanto region, in order to measure how slow slip at depth has been perturbed by the 2011 *M*9.0 main shock on both subducting plates. Following the work of *Kimura et al.* [2006], who identified clusters of REs at several locations on the Philippine Sea plate interface, we limit our study to their three areas that contain the most REs for their 1989–2003 period (areas F, G, and H, see Figure 1) but did not consider their area D [see *Kimura et al.*, 2006, Figure 3] which hosts the earthquake swarms related to the recurrent Boso slow slip event [*Hirose et al.*, 2012, 2014; *Ozawa*, 2014]. REs were found in these three areas at depths greater than 20 km, that are characteristic of the transition zone between the locked portion of the fault updip and the downdip freely slipping part. At these depths, low seismic coupling is found on the Philippine Sea plate [*Sagiya*, 2004; *Nishimura et al.*, 2007], possibly as a result of the mixture of asperities and invading creeping patches.

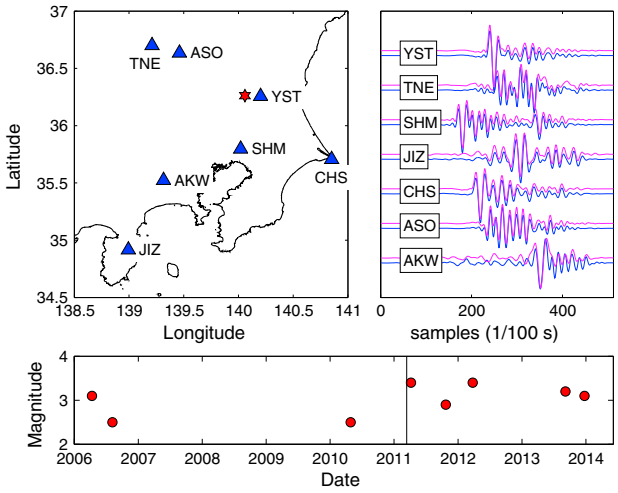

Figure 7. An example of two repeating earthquakes (9 April 2006 $M = 3.1$ and 4 April 2011 $M = 3.4$) with coherence greater than 0.9 at seven stations. The windowed 1.5–8 Hz band-pass filtered aligned normalized waveforms are shown for all seven stations. The time axis is arbitrarily offset from one station to the next, for better readability. (bottom) Occurrence times and magnitudes of the seven earthquakes forming the sequence which contains the 9 April 2006 and 4 April 2011 earthquakes. The vertical line marks the date of the *M*9.0 main shock.

We analyzed the waveforms of all $M \geq 1.0$, $z < 100$ km earthquakes from 2004 to June 2014, that are located in these three areas, as listed in the Japan Meteorological Agency data set, following a method derived from *Got et al.* [1994] and *Lengliné and Marsan* [2009]. Two minute long records sampled at 100 Hz of the vertical component at the closest 10 Hi-net stations were processed. For each pair of earthquakes and each recording station, the mean coherency in the 1.5 Hz–8 Hz band was computed, for a 512 sample-long window initially centered on the *P* wave arrival. Time delays were also computed in the same frequency band, by linearly fitting the coherency phase weighted by the coherency squared modulus. An iterative procedure that aligns the two waveforms and then recomputes the coherency and time delays on the new 512 sample-long windows allows to optimize the mean coherency and the accuracy of the estimated delay. We then selected all earthquake pairs characterized by a mean coherency greater than 0.9 for at least four stations, which is the minimum number in order to resolve the relative locations, by least squares fitting the time delays. Time delays are then used to compute the relative coordinates of the two earthquakes, each pair separately. We used the NIED velocity model to do so. We are here only interested in the distance d between each two earthquakes, for the pairs that passed the selection criterion. Rupture overlap is calculated by comparing d with the rupture radii L_1 and L_2 of the two earthquakes, with $L = (7M_o/16\Delta\sigma)^{1/3}$ [*Eshelby*, 1957], for a $\Delta\sigma = 30$ bar stress drop. For two earthquakes to be repeating instances of a nearly identical rupture, we require $d < \max\{L_1, L_2\}$, and their magnitudes to differ by 0.5 or less. This criterion is fundamental to make sure that two repeating earthquakes come from the same asperity. Indeed, only 10% of earthquakes that presented a mean coherency of 0.9 or more for at least four stations were really repeating earthquakes. We finally group together all pairs of REs that share a common earthquake and iterate until no earthquake belongs to distinct groups.

Figure 7 shows an example of two earthquakes (9 April 2006 $M = 3.1$ and 4 April 2011 $M = 3.4$) with aligned waveforms at the seven stations with mean coherency greater than 0.9. These two earthquakes are found to be distant by 96.5 ± 3.1 m and thus have a strong rupture overlap since $L_1 = 186$ m and $L_2 = 263$ m. An identical method, but based on the cross correlation of 1.5–8 Hz band-pass filtered waveforms rather than coherency, gives $d = 132 \pm 18$ m, which still corresponds to a strong overlap. These two earthquakes are part of an RE sequence that counts eight occurrences, see Figure 7. This sequence is clearly not periodic nor are the large majority of the other sequences. Perturbation by the 2011 *M*9.0 main shock can explain this nonperiodicity, but asperity interactions are likely to play a role too, as, for example, evidenced by the first two ruptures in this particular sequence, that occur in the pre-Tohoku period and are separated by only 116 days.

We find 105 RE sequences, grouping 355 earthquakes, with the largest sequence counting as many as 17 earthquakes. The sequences are approximately equally distributed on the two plates, see Figure 8. In order to capture a common trend in creeping rate, we stack the occurrence time series of all RE sequences separately for the two plates, cf. Figure 9. We checked that the cumulative slip (instead of cumulative number) time series follow very similar trends to these. Many stations among the 10 in our set were not operational before April 2006, which thus marks the beginning of the stable interseismic period we were able to resolve.

Following a sudden increase and subsequent relaxation after the *M*9.0 main shock, the REs located in the Pacific plate were still occurring in June 2014 at a rate 2.1 higher than the interseismic rate. This high rate

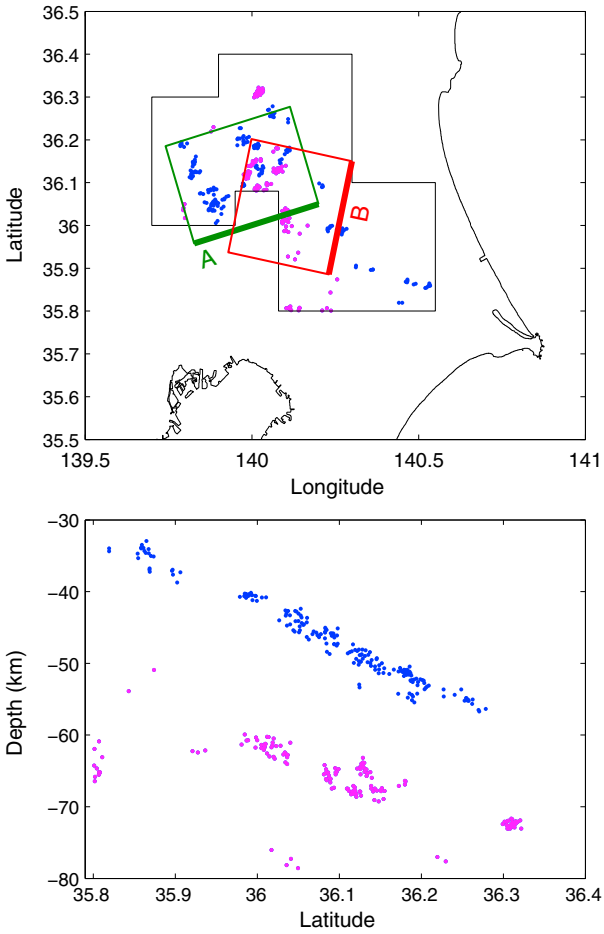

Figure 8. Map and cross section of the repeating earthquakes, color coded according to the plate they are located in. Only earthquakes within the dashed box are analyzed (areas F, G, and H of *Kimura et al.* [2006]). The two rectangular fault surfaces defined in section 4 are shown in green (fault A on PHS) and red (fault B on PAC); their upper limits are at 42 km and 60 km depth, respectively (thick lines).

has remained stationary for 1 year prior to this date. The ratio of 2.1 is robust when testing other RE selection criteria (i.e., by changing the minimum degree of rupture overlap and the magnitude difference).

In contrast, the RE occurrence rate in the Philippine Sea plate exhibits a clear relaxation following the initial increase after 11 March 2011. We fit this rate with an Omori-Utsu law with μ=15.8 per year for the interseismic RE rate. Two fits are computed: (1) the first by taking into account all RE occurrences between 11 March 2011 and June 2014 and (2) by fitting only the REs occurring between 11 March 2011 and 1 July 2012, which marks the beginning of a significant increase in rate, see Figure 9. According to these models, the rate increase ranges between +18% and +28% after 3 years and should decay quickly to a value ranging between +2.6% and +5.7% after 10 years (i.e., in 2021). These estimates indicate that the increase is much less than the current +110% increase experienced by the Pacific plate. Although there is a clear increase set after January 2014, more data are needed to see whether this is a long lasting increase or a short transient as in 11 July 2012.

An 80 day long increase is also observed from July to September 2012 for the Philippine Sea plate, that we could not relate to any evident cause like a strong, local shock, triggering extra seismic activity. During this time interval, only two REs occurred in the Pacific plate, which is an anomalously low number. This suggests that an increase in slip might have taken place on the Philippine Sea plate, with a slip rate 6 times higher than the interseismic rate according to our RE time series (hence, a total slip of 32 mm, taking the interseismic rate of 25 mm/year estimated for segment O in *Nishimura et al.* [2007]) and that it reduced the stressing rate on the deeper Pacific interface. Coulomb stress was computed with the source (with 32 mm slip) and receiver faults described in the following section. We find a Coulomb stress change of +0.012 bars. This very low stress change implies that direct mechanical interactions between the two plates are insignificant, at least with the small area of the PHS plate imaged by the locations of our REs. Finally, visual inspection of the GPS displacements at stations just above this area do not reveal any obvious sign of accelerated convergence during this period. Our source dislocation would generate a 0.7 mm (horizontal) and 3 mm (vertical) maximum surface displacement, which is about the measurement error of 1 day solution for GPS displacements.

4. Discussion

REs time series indicate that both plates have undergone accelerated creep in their transition zones at depth in the Kanto region. For the Pacific plate, which hosted the *M*9.0 rupture farther up North, this acceleration is still strong in 2014 and does not show any clear sign of relaxation as yet. We investigate whether this observation is consistent with static stress triggering. We model the geometry of the two areas in which we find REs: for REs on the PHS interface (fault A of Figure 8) we assume a 253° strike and 28.4° dip [*Kimura et al.*, 2006]. The Euler poles of *Nishimura et al.* [2007] then impose a rake angle of 87° for the 35 km × 30 km rectangular patch

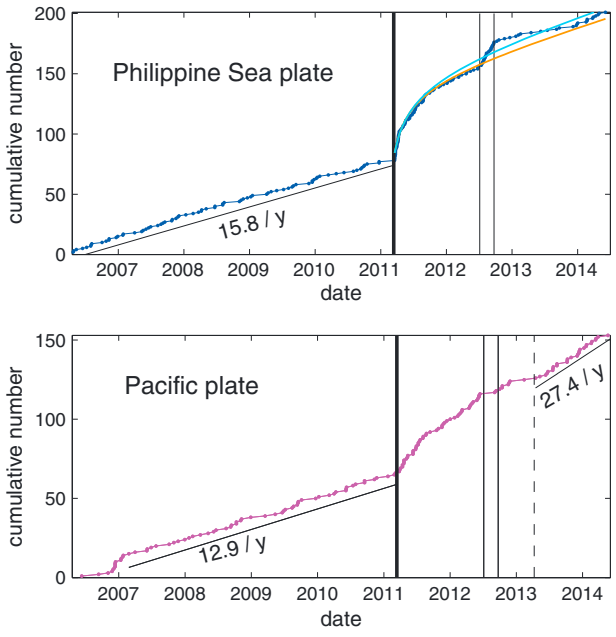

Figure 9. Repeating earthquakes time series, for the two plates taken separately. The occurrence date of the *M*9.0 Tohoku earthquake is indicated by a thick vertical line. Two Omori-Utsu laws are shown for the Philippine Sea plate when fitting from 11 March 2011 to 11 July 2012 (orange) and from 11 March 2011 to June 2014 (blue), see text. The 80 day long transient in rate (July to September 2012) is delimited for the two plates by the vertical lines.

that contains our REs, consistent with the almost pure inverse mechanisms of most REs found in this area by *Kimura et al.* [2006]. For REs on the PAC plate upper surface (fault B of Figure 8), we take the strike, dip, and rake angles of zone D of *Nishimura et al.* [2007], i.e., 192°, 23°, and 95°, respectively, and define a 30 km × 30 km fault surface.

We compute the change in Coulomb stress at the center of our two faults, for a friction coefficient of 0.4, that would result from 1 m of pure dip slip on individual triangular dislocations paving the Pacific plate surface. We used the same dislocations as *Perfettini and Avouac* [2014], that are based on the modeled plate surface of *Hayes et al.* [2012]. Almost all dislocations contribute positively to an increase in Coulomb stress on fault B (Figure 10b), except for two triangles very close to the fault due to errors and mismatch in geometrical modeling between the paving and our definition of fault B. This positive Coulomb stress changes are expected given the simple and regular geometry of the plate. For fault A located on the Philippine Sea plate, positive contributions are found for a roughly SSW-NNE trending band of the Pacific plate, cf. Figure 10a. The accelerated rate of REs on fault A thus implies that the coseismic slip distributions of the 2011 *M*9.0 main shock and of its immediate *M*7.9 aftershock just offshore Kanto preferentially occupy this band in the vicinity of fault A.

We calculated the change in Coulomb stress for three slip models of the 2011 ruptures: (1) the *Ide et al.* [2011] solution plus the *M*7.9 tapered slip dislocation of *Toda and Stein* [2013]; (2) the variable slip azimuth, and (3) the fixed slip azimuth solutions of *Perfettini and Avouac* [2014]. For cases (2) and (3), the slip corresponds to the

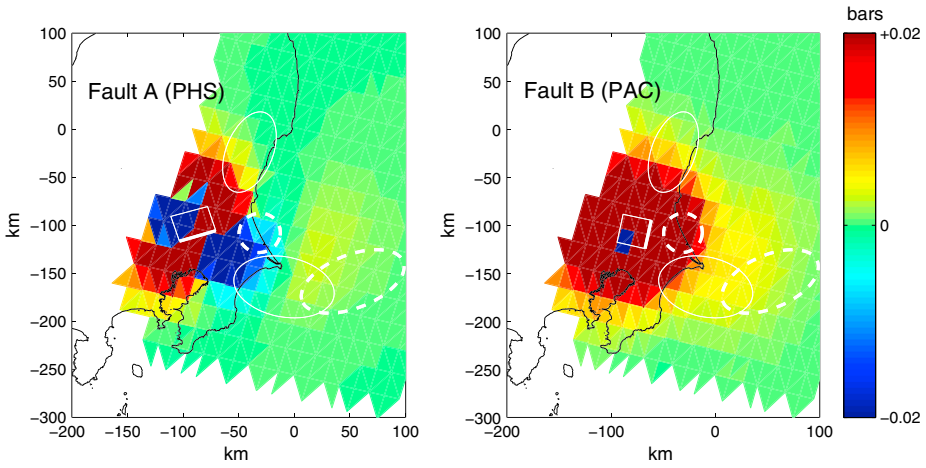

Figure 10. Coulomb stress change on (left) fault A and (right) fault B generated by triangular dislocations paving the PAC plate, for 1 m of dip slip for each dislocation. We map the value of this stress change created by a given triangular dislocation at the location of this triangle. The locations of maxima of afterslip are shown with thin white ellipses [*Perfettini and Avouac*, 2014] and with thick dashed white ellipses [*Ozawa et al.*, 2012].

Table 1. Coseismic Coulomb Stress Changes in Bars for a Friction Coefficient of 0.4, Calculated on Faults A and B[a]

Model	Fault A	Fault B
1	−0.15	1.42
2	1.02	0.87
3	0.28	1.03

[a] The three models are described in the text.

cumulative slip over 1 day, thus effectively including the *M*7.9 aftershock. Results are summarized in Table 1. The two models of *Perfettini and Avouac* [2014] are thus coherent with the observed rate increases on both faults A and B.

Afterslip on the Pacific slip interface is found south of the main rupture, as well evidenced by the clockwise rotation of GPS displacements in the Kanto region, compared to the coseismic displacements (Figure 6). Local maxima in the postseismic slip on PAC are effectively found both by *Ozawa et al.* [2012] and by *Perfettini and Avouac* [2014], albeit with differences in their exact locations, cf. Figure 10. These maxima yield from 0.8 to 1.1 m [*Perfettini and Avouac*, 2014] and from 1 m to less than 2 m [*Ozawa et al.*, 2012] of slip, for 279 days and 214 days, respectively. On top of this afterslip, slow slip on the Philippine Sea plate off Boso occurred at the end of October 2011 with a maximum slip of 0.3 m over about a week time [*Hirose et al.*, 2014].

Afterslip on PAC acts to further load fault B. On the contrary, fault A is unloaded by −0.43 to −0.13 bars for the variable and fixed slip azimuth solutions of *Perfettini and Avouac* [2014] and an unknown (but negative) amount for *Ozawa et al.* [2012] based on the location of the closest maximum in a strong negative contribution lobe, see Figure 10. This can explain why the rate of REs on fault A has decayed at a faster pace than on fault B. We moreover note that the RE time series on fault A exhibit, from the end of 2012 to the end of 2013, a rate lower than the pre-Tohoku rate, consistent with the unloading by afterslip (Figure 9).

We estimate how coseismic and postseismic slips, including accelerated creep on faults A and B, have affected stress on the locked portion of the Philippine Sea plate in Kanto. We compute the individual changes in Coulomb stress on the source of the 1923 *M*7.9 Kanto earthquake of *Matsu'ura and Iwasaki* [1983], for 1 m of dip slip on each triangular dislocation of the modeled PAC upper surface, see Figure 11. Coseismic slip acted to decrease failure stress on the fault by −0.005 bars for all three coseismic models, while postseismic slip, including accelerated creep on faults A and B, has the opposite effect of positively loading this fault: +0.019 bars (postseismic), +0.002 bars (creep on A after 1 year), and less than 0.001 bars (creep on B after 1 year). Moreover, the October 2011 off-Boso SSE also contributed to add +0.014 bars of Coulomb stress on this fault. These changes are all small and are averaged over the 95 km × 54 km fault surface. Larger changes are thus expected locally on the fault, although they remain modest; for example, the 2011 Boso SSE generated a maximum of +0.06 bars at the eastern tip of the fault. The stress changes on the 1923 Kanto earthquake fault caused by the 2011 main shock and subsequent slip events, are thus barely significant. They can, for example, be compared to the stressing rate corresponding to an earthquake cycle with 30 bars of stress drop and 500 years of return time, hence 0.06 bars/yr. The stress perturbations thus amount to less than a year of interseismic loading. This estimation, however, relies on the limited spatial extents of our faults A and B and on the strong uncertainties on both

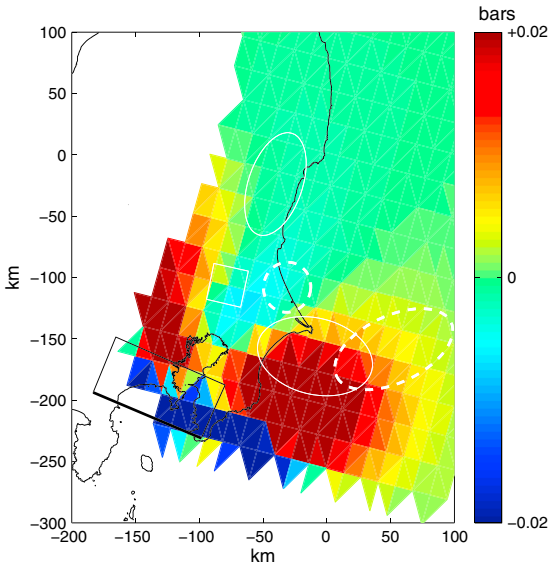

Figure 11. Same as Figure 10, but for the updip locked portion of the Philippine Sea plate that ruptured during the 1923 *M*7.9 earthquake (25° dip, 294° strike, and 144° rake; [*Matsu'ura and Iwasaki*, 1983]).

the return time and the stress drop of the characteristic Kanto earthquake. Accelerated creep on much larger surfaces would have a stronger impact in these stress calculations.

5. Conclusions

Following the 2011 *M*9.0 Tohoku earthquake, a remarkable increase in seismicity has affected the Kanto region. However, this increased activity has relaxed to pre-Tohoku rates on crustal faults and is in the process of doing so (as of June 2014) on deep sections of the Philippine Sea plate characterized by creep and repeating earthquakes. On the contrary, very little relaxation is observed on creeping portions of the Pacific plate; also, GPS inversions find secondary maxima of afterslip on this plate in the Kanto region. However, this acceleration of creep and silent slip, as well as direct coseismic effects, only less affect the stress state of the hypothesized source fault of the 1923 Kanto earthquake, that correspond to the strongly locked updip portion of the Philippine Sea plate in this region.

Acknowledgments
We would like to thank Shinji Toda and Hugo Perfettini for sharing their results, and Mark Simons and Francesco Ortega for preparing and providing us the GPS time series used in this study. Coulomb stress computations were performed using Coulomb3.0 and the triangular dislocation code of Brendan Meade. This work has benefited from financial support by the FP7 REAKT European project. Earthquake data were kindly provided by the Japan Meteorological Agency in cooperation with the Ministry of Education, Culture, Sports, Science and Technology. We acknowledge the help of the National Research Institute for Earth Science and Disaster Prevention, Tsukuba, for making available their waveform data through their website.

References

Bouchon, M., H. Karabulut, M. Aktar, S. Ozalaybey, J. Schmittbuhl, and M. P. Bouin (2011), Extended nucleation of the 1999 M_w 7.6 Izmit earthquake, *Science*, *331*(6019), 877–880, doi:10.1126/science.1197341.

Chen, K. H., R. M. Nadeau, and R. J. Rau (2007), Towards a universal rule on the recurrence interval scaling of repeating earthquakes?, *Geophys. Res. Lett.*, *34*, L16308, doi:10.1029/2007GL030554.

Eshelby, J. D. (1957), The determination of the elastic field of an ellipsoidal inclusion, and related problems, *Proc. R. Soc. London, Ser. A*, *241*, 376–396, doi:10.1098/rspa.1957.0133.

Got, J. L., J. Frechet, and F. W. Klein (1994), Deep fault plane geometry inferred from multiplet relative relocation beneath the south flank of Kilauea, *J. Geophys. Res.*, *99*, 15,375–15,386.

Hayes, G. P., D. J. Wald, and R. L. Johnson (2012), Slab1.0: A three-dimensional model of global subduction zone geometries, *J. Geophys. Res.*, *117*, B01302, doi:10.1029/2011JB008524.

Hirose, H., H. Kimura, B. Enescu, and S. Aoi (2012), Recurrent slow slip event likely hastened by the 2011 Tohoku earthquake, *Proc. Nat. Acad. Sci.*, *109*, 15,157–15,161.

Hirose, H., T. Matsuzawa, T. Kimura, and H. Kimura (2014), The Boso slow slip events in 2007 and 2011 as a driving process for the accompanying earthquake swarm, *Geophys. Res. Lett.*, *41*, 2778–2785, doi:10.1002/2014GL059791.

Ide, S., A. Baltay, and G. C. Beroza (2011), Shallow dynamic overshoot and energetic deep rupture in the 2011 Mw 9.0 Tohoku-Oki earthquake, *Science*, *332*(6036), 1426–1429.

Ishibe, T., K. Shimazaki, K. Satake, and H. Tsuruoka (2011), Change in seismicity beneath the Tokyo metropolitan area due to the 2011 off the Pacific coast of Tohoku Earthquake, *Earth Planets Space*, *63*, 731–735.

Ishida, M. (1992), Geometry and relative motion of the Philippine Sea plate and Pacific plate beneath the Kanto-Tokai District, Japan, *J. Geophys. Res.*, *97*, 489–513.

Kato, A., T. Igarashi, and K. Obara (2014), Detection of a hidden Boso slow slip event immediately after the 2011 M_w 9.0 Tohoku-Oki earthquake, Japan, *Geophys. Res. Lett.*, *41*, 5868–5874, doi:10.1002/2014GL061053.

Kimura, H., K. Kasahara, T. Igarashi, and N. Hirata (2006), Repeating earthquake activities associated with the Philippine Sea plate subduction in the Kanto district, central Japan: A new plate configuration revealed by interplate aseismic slips, *Tectonophysics*, *417*, 101–118.

Lengliné, O., and D. Marsan (2009), Inferring the coseismic and postseismic stress changes caused by the 2004 $M_w = 6$ Parkfield earthquake from variations of recurrence times of microearthquakes, *J. Geophys. Res.*, *114*, B10303, doi:10.1029/2008JB006118.

Marsan, D., E. Prono, and A. Helmstetter (2013), Monitoring aseismic forcing in fault zones using earthquake time series, *Bull. Seismol. Soc. Am.*, *103*, 169–179.

Matsu'ura, M., and T. Iwasaki (1983), Study on coseismic and postseismic crustal movements associated with the 1923 Kanto earthquake, *Tectonophysics*, *97*, 201–215.

Matsuzawa, T., T. Igarashi, and A. Hasegawa (2002), Characteristic small-earthquake sequence off Sanriku, northeastern Honshu, Japan, *Geophys. Res. Lett.*, *29*(11), 38–1–38-4, doi:10.1029/2001GL014632.

Nadeau, R. M., W. Foxall, and T. V. McEvilly (1995), Clustering and periodic recurrence of microearthquakes on the San Andreas fault at Parkfield, California, *Science*, *267*, 503–507.

Nadeau, R. M., and T. V. McEvilly (1999), Fault slip rates at depth from recurrence intervals of repeating microearthquakes, *Science*, *285*, 718–721.

Nanjo, K. Z., S. Sakai, A. Kato, H. Tsuruoka, and N. Hirata (2013), Time-dependent earthquake probability calculations for southern Kanto after the 2011 *M*9.0 Tohoku earthquake, *Geophys. J. Int.*, *193*, 914–919, doi:10.1093/gji/ggt009.

Nishimura, T., T. Sagiya, and R. S. Stein (2007), Crustal block kinematics and seismic potential of the northernmost Philippine Sea plate and Izu microplate, central Japan, inferred from GPS and leveling data, *J. Geophys. Res.*, *112*, B05414, doi:10.1029/2005JB004102.

Ozawa, S., T. Nishimura, H. Suito, T. Kobayashi, M. Tobita, and T. Imakiire (2011), Coseismic and postseismic slip of the 2011 magnitude-9 Tohoku-Oki earthquake, *Nature*, *475*, 373–376, doi:10.1038/nature10227.

Ozawa, S., T. Nishimura, H. Munekane, H. Suito, T. Kobayashi, M. Tobita, and T. Imakiire (2012), Preceding, coseismic, and postseismic slips of the 2011 Tohoku earthquake, Japan, *J. Geophys. Res.*, *117*, B07404, doi:10.1029/2011JB009120.

Ozawa, S. (2014), Shortening of recurrence interval of Boso slow slip events in Japan, *Geophys. Res. Lett.*, *41*, 2762–2768, doi:10.1002/2014GL060072.

Perfettini, H., and J. P. Avouac (2014), The seismic cycle in the area of the 2011 M_w9.0 Tohoku-Oki earthquake, *J. Geophys. Res. Solid Earth*, *119*, 4469–4515, doi:10.1002/2013JB010697.

Sagiya, T. (2004), Interplate coupling in the Kanto District, Central Japan, and the Boso Peninsula Silent Earthquake in May 1996, *Pure Appl. Geophys.*, *161*, 2317–2342.

Schaff, D. P., G. C. Beroza, and B. E. Shaw (1998), Postseismic response of repeating aftershocks, *Geophys. Res. Lett.*, *25*, 4549–4552.

Somerville, P. G. (2014), A post-Tohoku earthquake review of earthquake probabilities in the southern Kanto District, Japan, *Geosci. Lett.*, *1*, 1–13.

Sun, T., et al. (2014), Prevalence of viscoelastic relaxation after the 2011 Tohoku-oki earthquake, *Nature*, *514*, 84–87, doi:10.1038/nature13788.

Toda, S., and R. S. Stein (2013), The 2011 $M = 9.0$ Tohoku-oki earthquake more than doubled the probability of large shocks beneath Tokyo, *Geophys. Res. Lett.*, *40*, 2562–2566, doi:10.1002/grl.50524.

Uchida, N., and T. Matsuzawa (2013), Pre- and postseismic slow slip surrounding the 2011 Tohoku-oki earthquake rupture, *Earth Planet. Sci. Lett.*, *374*, 81–91.

Uchida, N., J. Nakajima, A. Hasegawa, and T. Matsuzawa (2009), What controls interplate coupling: Evidence for abrupt change in coupling across a border between two overlying plates in the NE Japan subduction zone, *Earth Planet. Sci. Lett.*, *283*, 111–121.

Uchida, N., S. Shimamura, T. Matsuzawa, and T. Okada (2015), Postseismic response of repeating earthquakes around the 2011 Tohoku-oki earthquake: Moment increases due to the fast loading rate, *J. Geophys. Res. Solid Earth*, *120*, 259–274, doi:10.1002/2013JB010933.

Watanabe, S., M. Sato, M. Fujita, T. Ishikawa, Y. Yokota, N. Ujihara, and A. Asada (2014), Evidence of viscoelastic deformation following the 2011 Tohoku-Oki earthquake revealed from seafloor geodetic observation, *Geophys. Res. Lett.*, *41*, 5789–5796, doi:10.1002/2014GL061134.

Wu, F., D. Okaya, H. Sato, and N. Hirata (2007), Interaction between two subducting plates under Tokyo and its possible effects on seismic hazards, *Geophys. Res. Lett.*, *34*, L18301, doi:10.1029/2007GL030763.